

# A high oxidation resistance Ti<sub>2</sub>AlC coating on Zirlo substrates for loss-of-coolant accident conditions



Wentao Li<sup>a</sup>, Zhenyu Wang<sup>a</sup>, Jintao Shuai<sup>a</sup>, Beibei Xu<sup>a</sup>, Aiyong Wang<sup>a,b,\*\*</sup>, Peiling Ke<sup>a,b,\*</sup>

<sup>a</sup> Key Laboratory of Marine Materials and Related Technologies, Zhejiang Key Laboratory of Marine Materials and Protective Technologies, Ningbo Institute of Materials Technology and Engineering, Chinese Academy of Sciences, Ningbo, 315201, China

<sup>b</sup> Center of Materials Science and Optoelectronics Engineering, University of Chinese Academy of Sciences, Beijing, 100049, China

## ARTICLE INFO

### Keywords:

Ti<sub>2</sub>AlC  
MAX phase coating  
Oxidation resistance  
ATFs cladding

## ABSTRACT

After Fukushima nuclear accident, the concept of ATFs cladding coating was proposed in order to provide more rescue time under accident conditions. In this work, we fabricated the dense Ti<sub>2</sub>AlC MAX phase coatings on Zirlo substrate using a hybrid arc/magnetron sputtering technique followed by an annealing treatment. Mechanical properties of the Ti<sub>2</sub>AlC coating was evaluated, and its oxidation resistance in pure steam conditions was particularly investigated at 1000 °C, 1100 °C and 1200 °C under different oxidation times. The results showed that Ti<sub>2</sub>AlC coating presents the higher hardness and elastic modulus than substrate, which can effectively improve the mechanical properties of bare Zirlo substrates. The high-temperature oxidation resistance of the Zirlo substrate in pure steam was significantly improved by the coatings with a compact structure and the formed triple scale oxide scale (α-Al<sub>2</sub>O<sub>3</sub> + R-TiO<sub>2</sub>/α-Al<sub>2</sub>O<sub>3</sub>/TiO<sub>2</sub>) during oxidation process. The presented Ti<sub>2</sub>AlC MAX phase coatings with a facile hybrid arc/sputtering technique enable them a promising candidate as oxidation protective coatings for ATF claddings.

## 1. Introduction

Due to low thermal neutron absorption cross-section, outstanding mechanical properties and relative good corrosion resistance under harsh conditions, Zirconium alloys fuel cladding, like Zircaloy-4, M5 and Zirlo, have been extensively used in light water reactors (LWRs) [1]. However, the reaction between zirconium and steam at high temperature is accompanied by the release of large amounts of hydrogen gas, which leads to serious consequences, such as the Fukushima nuclear accident [2]. Surface coatings are considered to be a more reliable and cost-efficient strategy to improve the safety of accident tolerant fuels (ATFs), which can separate the reaction between steam and zirconium, so as to delay and even avoid accidents.

Generally, it is empirically required that ATFs cladding coatings should exhibit certain strength, good neutron irradiation resistance and excellent oxidation resistance in high temperature steam atmosphere [3]. A great deal of work investigating ATF cladding coating preparation and optimizing their properties have been done over the past few decades, which include SiC coatings [4,5], Cr coatings [6], FeCrAl

coatings [7], AlCrMoNbZr HEA coatings [8], and M<sub>n+1</sub>AX<sub>n</sub> phases (referred to as MAX phases) coatings [9,10], where the formed Cr<sub>2</sub>O<sub>3</sub>, Al<sub>2</sub>O<sub>3</sub> and SiO<sub>2</sub> enable the oxidation resistance even up to 1000 °C, 1400 °C and 1700 °C, respectively [11]. Different with other candidates, MAX phases are nano-laminated ternary ceramics, in which M stands for an early transition metal, A is an IIIA- or IVA-group element, and X is either carbon or/and nitrogen. They have unique properties that combine the merits of both metals and ceramics [12,13] for high temperature applications and neutron activation, which are similar to SiC and three orders of magnitude less than Alloy 617 after 10–60 years [14]. Nevertheless, the oxidation resistance is strongly dependent upon the thickness and structure of coatings, the exposure working environment, and the desired lifetime, etc.

Ti<sub>2</sub>AlC belongs to a family of MAX phase and has lower thermal expansion coefficient, better thermal shock resistance and higher temperature oxidation resistance, especially its excellent stability under neutron irradiation [14,15]. Basu et al. [16] has investigated the long-term oxidation behavior of Ti<sub>2</sub>AlC bulk materials in air and steam at 1000–1300 °C. They found that here were a formed continuous Al<sub>2</sub>O<sub>3</sub>

\* Corresponding author. Key Laboratory of Marine Materials and Related Technologies, Zhejiang Key Laboratory of Marine Materials and Protective Technologies, Ningbo Institute of Materials Technology and Engineering, Chinese Academy of Sciences, Ningbo, 315201, China.

\*\* Corresponding authors. Key Laboratory of Marine Materials and Related Technologies, Zhejiang Key Laboratory of Marine Materials and Protective Technologies, Ningbo Institute of Materials Technology and Engineering, Chinese Academy of Sciences, Ningbo, 315201, China.

E-mail addresses: [aywang@nimte.ac.cn](mailto:aywang@nimte.ac.cn) (A. Wang), [kepl@nimte.ac.cn](mailto:kepl@nimte.ac.cn) (P. Ke).

<https://doi.org/10.1016/j.ceramint.2019.04.089>

Received 2 January 2019; Received in revised form 20 March 2019; Accepted 10 April 2019

Available online 22 April 2019

0272-8842/ © 2019 Elsevier Ltd and Techna Group S.r.l. All rights reserved.

scale with a thin scale of  $\text{TiO}_2$  on the top surface, in which the  $\text{Al}_2\text{O}_3$  scale provided excellent protection from further oxidation and adhered well to the  $\text{Ti}_2\text{AlC}$  substrate, due to the matching thermal expansion. Furthermore, Tang et al. [17] demonstrated the maximum tolerant temperature of  $\text{Ti}_2\text{AlC}$  in steam could reach about  $1555^\circ\text{C}$ . Taking into account the differences of properties between bulk materials and coating candidates. Various deposition processes have recently been adopted to prepare  $\text{Ti}_2\text{AlC}$  coating or film on Zirconium alloy, including cold spray [18], magnetron sputtering followed by thermal annealing [19–21]. For example, Wang et al. [22] investigated the oxidation behavior of Ti–Al–C films mainly composed of  $\text{Ti}_2\text{AlC}$  phase at  $800^\circ\text{C}$  and  $900^\circ\text{C}$ , and found that the  $\text{Ti}_2\text{AlC}$  phase was quickly consumed during oxidation, and three oxidation scales were observed, including outer  $\text{TiO}_2$ -rich scale, middle  $\text{Al}_2\text{O}_3$ -rich scale, and inner  $\text{TiO}_2 + \text{Al}_2\text{O}_3$  mixed scale. Benjamin et al. [23] studied the oxidation resistance performance of  $\text{Ti}_2\text{AlC}$ -coated Zry-4 alloys by simulating Loss of Coolant Accident (LOCA) tests at  $1005^\circ\text{C}$  in steam environment followed by a water quench. They showed that  $\text{Ti}_2\text{AlC}$  coatings provided effective protection to the underlying Zircaloy-4 alloy after 20 min oxidation. However, structure of the coating was loose and the longer oxidation time was not involved. Tang et al. [24] systematically studied the oxidation resistance behavior of  $\text{Ti}_2\text{AlC}$ -coated Zircaloy-4 in high-temperature steam from  $800^\circ\text{C}$  to  $1200^\circ\text{C}$ , in which the coatings were rapidly oxidized and showed only slightly protection around  $1000^\circ\text{C}$ . Overall, the superior oxidation resistance of bulk  $\text{Ti}_2\text{AlC}$  was not inherited by the coatings due to the formed structure defects.

In general, structure of the cold sprayed coatings is loose; while coatings prepared by magnetron sputtering, with low deposition rate, and usually have open columnar structure. In terms of reported results on oxidation resistance,  $\text{Ti}_2\text{AlC}$  coatings present excellent oxidation resistance at temperature lower than  $900^\circ\text{C}$ , mainly due to the formation of continuous and compact  $\text{Al}_2\text{O}_3$  scale during oxidation process. However, the evolution on oxidation resistance at high temperature ( $> 900^\circ\text{C}$ ) are still lack of study, and especially the mechanism in steam condition has not been fully understood yet.

In our previous work [25], an advanced hybrid technique based on the combined arc/sputtering method was developed to prepare the MAX (A = Al) phase coatings. The obtained  $\text{Ti}_2\text{AlN}$  MAX phase coatings by this technique have been characterized by compactness, high stability, super thickness and less few arc particles, comparing with those deposited by conventional magnetron sputtering or arc ion plating [26]. Motivated by this technique, furthermore, we fabricated the  $\text{Ti}_2\text{AlC}$  MAX phase coatings together with extended annealing treatment. The oxidation resistance properties of the  $\text{Ti}_2\text{AlC}$  coating under pure steam conditions at  $1000^\circ\text{C}$ ,  $1100^\circ\text{C}$  and  $1200^\circ\text{C}$  for different oxidation time were focused in this work. Finally, the related oxidation mechanism was discussed in terms of the structural evolution during oxidation process.

## 2. Experimental procedure

Zirlo alloys with size of  $15\text{ mm} \times 10\text{ mm} \times 2\text{ mm}$ , finding their major application in nuclear fuel cladding material, were chosen as the substrates. The nominal composition of the alloy in weight percent is Sn, 1.0, Nb, 1.0, Fe, 0.1 and the balance Zr. Initially, the Ti–Al–C coatings were deposited on the substrate by a hybrid arc/magnetron sputtering method. Schematic diagram of the deposition experiment arrangement is illustrated in Fig. 1. The circular titanium target (Ti, purity of 99.9%) and rectangular aluminum target (Al, purity of 99.9%) were used as the arc cathode source and sputtering source, respectively. Prior to deposition, the Zirlo alloy substrates were polished to 3000-grit by silicon carbon paper, and ultrasonically cleaned in acetone and ethanol each for 15 min. Then, the samples were hung on fixture directly facing the sputtering target. The chamber was pumped down to a base pressure below  $3.0 \times 10^{-5}$  Torr in order to eliminate foreign gas. To ensure all the substrate faces were coated, the deposition process

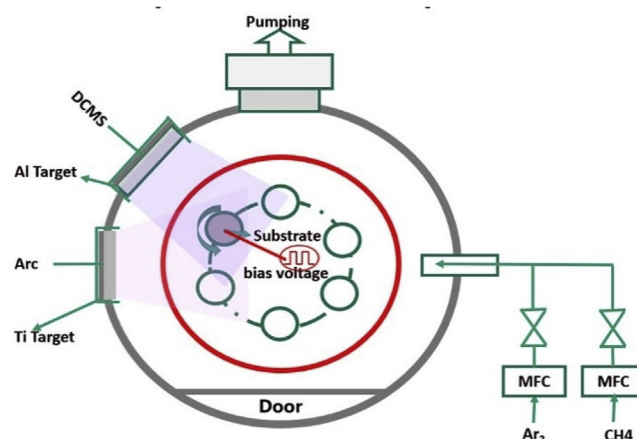


Fig. 1. Schematic diagram of the experiment arrangement.

was in the manner of rotation. The flux of Ar (purity, 99.999%) and  $\text{CH}_4$  (purity, 99.999%) were 200 sccm and 15 sccm, respectively, with the working pressure of 30 mTorr by controlling the valve of the vacuum chamber. In order to avoid diffusion of elements, a TiC diffusion barrier about  $1.5\ \mu\text{m}$  was deposited onto the substrate. The arc power was controlled at 17 W and the sputter power was controlled at 3.1 kW. The DC negative bias voltage of  $-200\text{ V}$  was applied to the substrates without other intentional heating. More detailed deposition parameters of the Ti–Al–C coatings can be found in our previous articles [27].

After 120 min deposition, the annealing treatment of as-deposited Ti–Al–C coating was conducted at  $600^\circ\text{C}$  for 50 h to obtain the  $\text{Ti}_2\text{AlC}$  MAX phase, and the heating rates was fixed at  $5\text{ K/min}$ . Before the annealing process, the tube furnace was firstly pumped down to  $-0.1\text{ MPa}$  and then filled with Ar (purity, 99.999%). In order to remove the residual air, the procedure was repeated three times. Then, the furnace temperature increased to preset value.

The performance of high-temperature steam oxidation resistance of bare and  $\text{Ti}_2\text{AlC}$ -coated Zirlo alloy was examined using home-made steam generator and heat treatment furnace. The weight changes before and after oxidation were weighed by electronic balance, and the accuracy is 0.01 mg. Before oxidation test, all samples were kept in an oven at  $200^\circ\text{C}$ .

The cross-section and surface morphology of the  $\text{Ti}_2\text{AlC}$  coatings before and after oxidation were characterized by scanning electron microscopy (SEM, FEI Quanta FEG 250) equipped with energy dispersive X-ray spectroscopy (EDS, Oxford X-Max). The crystal structure of oxide formed during the high-temperature oxidation test was analyzed by X-ray diffraction (XRD), with a BrukerD8 Advance diffractometer using  $\text{Cu K}\alpha$  radiation. To evaluate the hardness and elastic modulus of the coatings, MTS-G200 nanoindenter with a continuous stiff model was used. The representative hardness of the coating was selected in the depth of 1200 nm to avoid the effect caused by the substrate, and samples were mirror polished before nanoindentation measurements. Raman spectroscopy were performed to identify the microstructure evolution before and after annealing as it represented a sensitive tool for carbon-containing materials. X-ray photoelectron spectroscopy (XPS, Thermo Scientific ESCALAB 250) with Al ( $\text{mono}$ )  $\text{K}\alpha$  irradiation at pass energy of 160 eV was used to analyze the composition and chemical bonds of the surface oxidation products. Hardness and elastic modulus were evaluated in a nanoindentation tester (MTS G200) using a Berkovich indenter with the continuous stiffness mode and Oliver-Pharr method [28], and the indentation depth was about 10% of the coating thickness to avoid the substrate effects. Ten repeated measurements were carried out to minimize the measurement error.

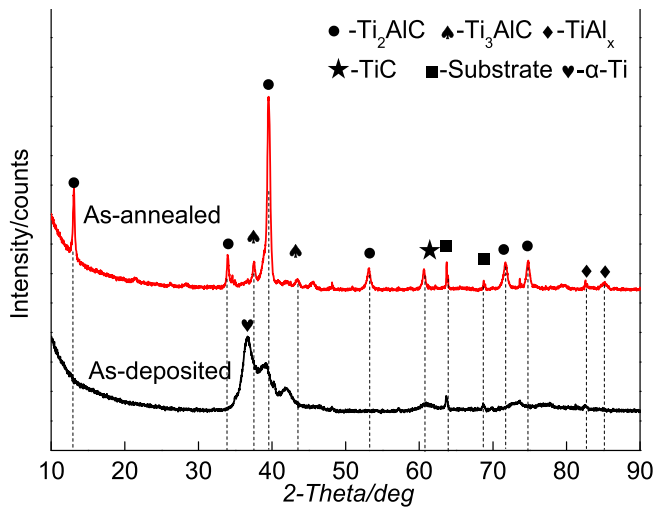


Fig. 2. X-ray diffraction pattern of the as-deposited and annealed Ti–Al–C coated Zirlo alloy.

### 3. Results and discussion

#### 3.1. Characterization of the coatings

##### 3.1.1. Composition and structure

X-ray diffraction patterns of both the as-deposited and annealed Ti–Al–C coated Zirlo alloy are shown in Fig. 2. The as-deposited Ti–Al–C coating is mainly composed of hexagonal Ti (103), which is recorded as  $\alpha$ -Ti. After annealing at 600 °C for 50 h, in addition to a small amount of diffraction peaks of substrate, three kinds of peaks with many TiC, Ti<sub>3</sub>AlC and Ti<sub>2</sub>AlC MAX phase appear. This indicates that Ti<sub>2</sub>AlC phase has been formed and there are a small amount of TiC (200), Ti<sub>3</sub>AlC (111) and Ti<sub>3</sub>AlC (200) impurity phases. In addition, the formed Ti<sub>2</sub>AlC MAX phase coating illustrates a good crystallinity according to the shown high and sharp diffraction peaks of Ti<sub>2</sub>AlC. Similar results are also found in our previous work, where the formation of Ti<sub>2</sub>AlC MAX phase is diffusion-controlled crystallization and growth processes [27].

Raman spectroscopy is a powerful technique for characterizing Ti<sub>2</sub>AlC MAX phase compounds, as there are four Raman active modes ( $2E_{2g}$ ,  $E_{1g}$  and  $A_{1g}$  at 153 cm<sup>-1</sup>, 260.9 cm<sup>-1</sup>, 270.3 cm<sup>-1</sup> and 365.1 cm<sup>-1</sup>) within the 211 phases [29]. As shown in Fig. 3, no Raman

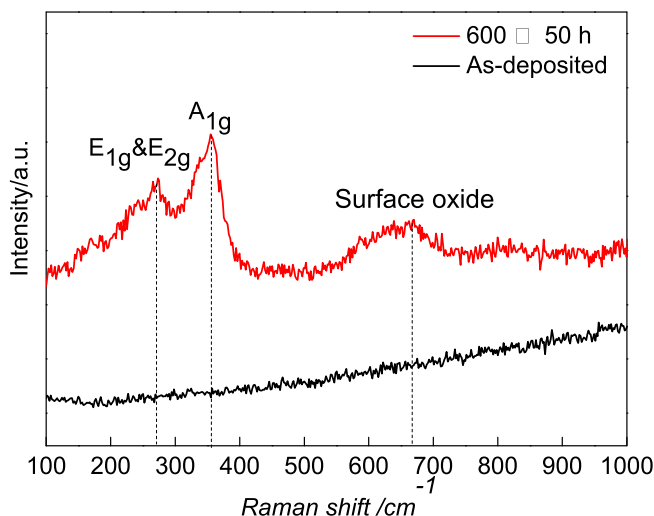


Fig. 3. Raman spectra of the as-deposited and annealed Ti–Al–C coated Zirlo substrate.

activity can be visible for the deposited Ti–Al–C coatings, while the annealed one shows two peaks at  $E_{1g}E_{2g} \sim 275$  cm<sup>-1</sup> and  $A_{1g} \sim 364$  cm<sup>-1</sup> corresponding to the first-order vibration peaks of Ti<sub>2</sub>AlC, which is consistent with previous literature [29]. Noted that a weaker band located at around 680 cm<sup>-1</sup> is also observed due to the formed thin surface oxide and/or oxycarbide scale [19]. Such Raman results further confirm the formation of Ti<sub>2</sub>AlC phase.

Fig. 4 shows the surface and cross-section morphology of the annealed coating. As shown in Fig. 4a, the as-annealed coating exhibits compact microstructure, except for some maroparticles and pits displayed in the coating surface (Fig. 4b), which is a typical feature of hybrid arc/magnetron sputtering deposition [25]. The maroparticles are mainly attributed to the ejected liquid droplets from the Ti target during arc discharge, while the formation of pits is mainly due to the exfoliation of some large particles during the deposition process. Nevertheless, it is interesting to note that the annealed coating exhibits a uniform, compact and defect-free structure from the cross-section morphology (Fig. 4c). Meanwhile,  $\sim 1.5$   $\mu$ m thick inner TiC adhesive scale and  $\sim 12.0$   $\mu$ m thick outer Ti<sub>2</sub>AlC scale are distinctly identified, which is in a relatively ideal thickness range for ceramic coatings [30]. Owing to the existence of TiC diffusion barrier, the interface structure of the coating is clear, indicating that there is no obvious mutual diffusion between the substrate and the coating. The results can also be proved by the corresponding EDX line scan for elemental composition (Fig. 4d) along the yellow line in Fig. 4c.

##### 3.1.2. Mechanical properties

Table 1 shows the hardness (H) and elastic modulus (E) of annealed Ti–Al–C coatings and Zirlo substrate. The Zirlo substrate is proved to be relatively soft, and the H and E are  $5.4 \pm 0.1$  GPa and  $129.9 \pm 3.1$  GPa, respectively. However, the Ti<sub>2</sub>AlC coated Zirlo substrate presents the higher H and E, namely, around 14.3 GPa for hardness and 230.8 GPa for elastic modulus. The H is almost at three times of those for Zirlo alloy substrate. Considering that elastic strain to failure (H/E) [31] and plastic strain to failure ( $H^3/E^2$ ) [32] play an important role in wear control and resistance of plastic deformation, respectively, the H/E (0.06) and  $H^3/E^2$  (0.05) of the Ti<sub>2</sub>AlC coating is also relatively high compared with those of the substrate material. In this case, it could be said that Ti<sub>2</sub>AlC coating can effectively improve the mechanical properties of bare zirconium alloy substrates.

#### 3.2. Isothermal oxidation behavior

The oxidation resistance of Ti<sub>2</sub>AlC coated Zirlo substrates was systematically tested at 1000–1200 °C in steam to evaluate the vapor oxidation resistance of Ti<sub>2</sub>AlC coatings under LOCA conditions.

##### 3.2.1. 1000 °C oxidation resistance in steam

Fig. 5 presents the morphology evolution of the Ti<sub>2</sub>AlC coated Zirlo substrates after oxidation in steam at 1000 °C for different oxidation time, using bare Zirlo substrate as a reference. After oxidation at 1000 °C for 10 min and 20 min, the adhesion between the coating and substrate is good and no coating spalling is found. The weight gain is 0.13 g/cm<sup>2</sup> and 1.96 g/cm<sup>2</sup>, respectively. However, macroscopic cracks begin to appear on the coating surface when the oxidation time prolongs to 30 min. Meanwhile, the oxidation weight gain increases to 5.90 g/cm<sup>2</sup>. It indicates that the oxidation degree of Ti<sub>2</sub>AlC coating is increased gradually with prolonging the oxidation time. Nevertheless, the coating still does not peel off, and the weight gain of Ti<sub>2</sub>AlC-coated Zirlo is significantly reduced compared with that of bare Zirlo (2.11 g/cm<sup>2</sup>) at 1000 °C for 10 min.

Fig. 6 shows surface morphologies of Ti<sub>2</sub>AlC-coated Zirlo after oxidation at 1000 °C. After oxidation for 10 min, the coating is slightly oxidized. Nevertheless, oxidation at maroparticles is more severe than elsewhere in the coating. Since the maroparticles are in Ti-rich, it is more likely that TiO<sub>2</sub> has been generated there. When the oxidation

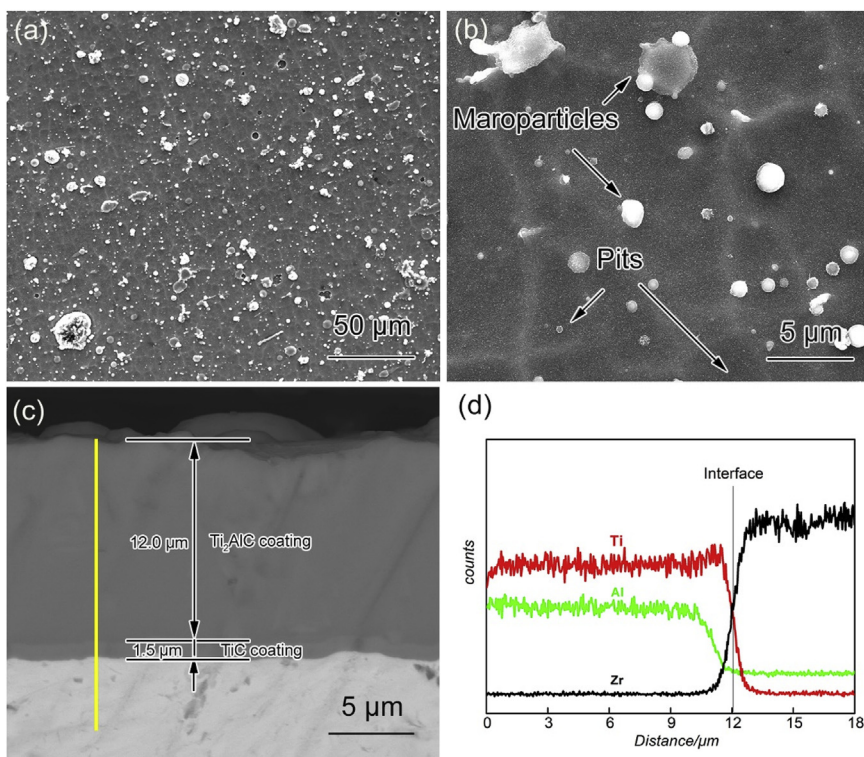


**Fig. 4.** SEM images of (a) surface of as-annealed coating at low magnification, (b) at high magnification, (c) cross-section, (d) the corresponding EDX line scan along the yellow line in (c). (For interpretation of the references to colour in this figure legend, the reader is referred to the Web version of this article.)

**Table 1**  
Mechanical properties of substrate and Ti<sub>2</sub>AlC coating.

	Hardness (GPa)	Elastic Modulus (GPa)	H/E	H <sup>3</sup> /E <sup>2</sup> (GPa)
Substrate	5.39 ± 0.1	129.92 ± 3.1	0.04	0.01
Ti <sub>2</sub> AlC coating	14.25 ± 0.1	230.8 ± 3.1	0.06	0.05

time increases to 20 min, the coating is obviously oxidized in large area and produced massive oxidation products, which are typical morphology of Rutile-TiO<sub>2</sub> (R-TiO<sub>2</sub>) [33]. The grain size of R-TiO<sub>2</sub> further increases and long strip-like of R-TiO<sub>2</sub> grains appear at oxidation for 30 min. It can be seen from the above results that increasing the prolongation of oxidation time leads to the increased oxidation of the coating.

To further confirm the oxidation products on the surface of the coatings in Fig. 6, XPS measurements, as presented in Fig. 7, were conducted for the coatings after oxidation at 1000 °C for 10 min and

20 min, which displays the spectra of Ti, Al and C of the oxidized coatings. Because of the limited detection range of XPS, there is no obvious change in the XPS results after oxidation at 1000 °C for 10 min and 20 min. There are two components in Ti 2p spectra of Ti<sub>2</sub>AlC coating oxidized at 1000 °C: Ti 2p<sub>3/2</sub> peaks in the oxide located at around 464.2 eV and 456.3 eV are identified as R-TiO<sub>2</sub> and TiO, respectively. Al 2p peaks in the oxide located at around 75.2 eV are related to metastable α-Al<sub>2</sub>O<sub>3</sub> [24]. Therefore, the O1s band could be decomposed into two components: one at 531.0 eV is ascribed to TiO<sub>2</sub> and Ti<sub>2</sub>O<sub>3</sub> oxides, and the other at 532.2 eV which is assigned to α-Al<sub>2</sub>O<sub>3</sub>. The results indicate that the surface can be mainly composed of a mixture of R-TiO<sub>2</sub> with a small amount of Ti<sub>2</sub>O<sub>3</sub> and α-Al<sub>2</sub>O<sub>3</sub>, which is consistent with SEM results.

Fig. 8 shows X-ray diffraction (XRD) pattern of Ti<sub>2</sub>AlC-coated Zirlo after oxidation at 1000 °C for 10 min, 20 min and 30 min. After oxidation for 10 min, the main diffraction peaks are Ti<sub>2</sub>AlC phase with a few of the diffraction peaks of rutile (R-TiO<sub>2</sub>) and α-Al<sub>2</sub>O<sub>3</sub>. It can be concluded that the Ti<sub>2</sub>AlC coating react with steam and are oxidized,

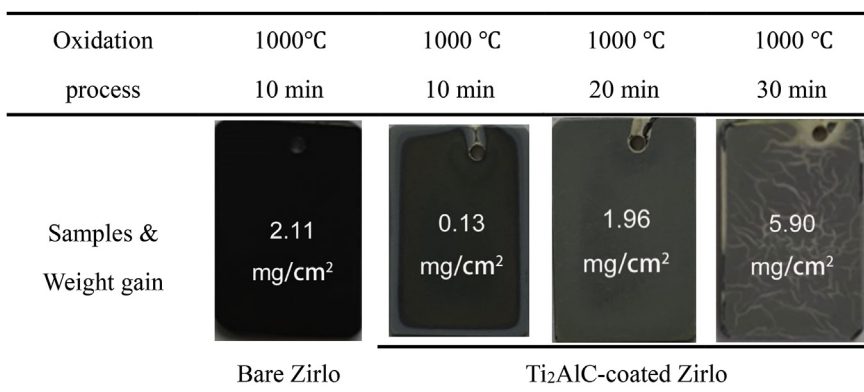


**Fig. 5.** Surface photos of the samples after isothermal oxidation in steam at 1000 °C for different times with corresponding change of the oxidation weight gain.

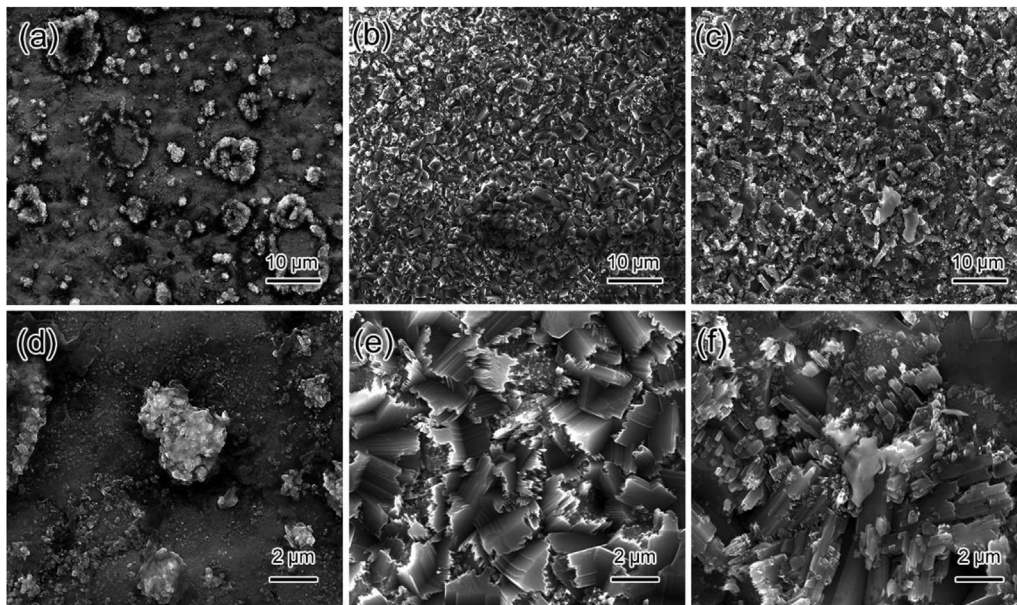


Fig. 6. Surface morphologies of the samples after isothermal oxidation in steam at 1000 °C for 10 min (a), 20 min (b) and 30 min (c) with at high magnification (d), (e) and (f).

forming the oxides of R-TiO<sub>2</sub> and α-Al<sub>2</sub>O<sub>3</sub>. When the oxidation time increase to 20 min, the diffraction peaks of Ti<sub>2</sub>AlC phase decrease and even disappear, and the diffraction peaks are mainly related to R-TiO<sub>2</sub>, indicating that the Ti<sub>2</sub>AlC coating is seriously oxidized. However, due to the limitation of XRD detection scope, no more Ti<sub>2</sub>AlC phases were noticed at this time.

When the coating is oxidized at 1000 °C for 30 min, the diffraction peak of Ti<sub>2</sub>AlC phase is further reduced, accompanied with the enhanced diffraction peak of R-TiO<sub>2</sub> phase, which means that the Ti<sub>2</sub>AlC coating is gradually oxidized and produced more oxidation products. Moreover, the crystallinity of the R-TiO<sub>2</sub> oxide is also enhanced. The XRD results show that the oxidation of Ti<sub>2</sub>AlC coatings will be aggravated with the increase of oxidation time.

The cross-section morphologies of both bare and Ti<sub>2</sub>AlC-coated Zirlo substrate oxidized at 1000 °C for 10 min are investigated using SEM and

EDS, as shown in Fig. 9. Serious oxidation takes place on the bare Zirlo, and the thickness of ZrO<sub>2</sub> oxide layer is ~10.8 μm, as proved by Fig. 9a with corresponding O elemental mapping (Fig. 9c). According to the EDS elemental mapping results (Fig. 9d), it is found that the Ti<sub>2</sub>AlC-coated Zirlo was slightly oxidized at same conditions. There is only a thin O enrichment zone on the surface of the coating and no obvious diffusion phenomenon occurs at the interface between the coating and Zirlo substrate. Tang et al. [24] concluded that Ti<sub>2</sub>AlC coating prepared by magnetron sputtering with annealing had very poor resistance to vapor oxidation at temperatures higher than 1000 °C. However, the Ti<sub>2</sub>AlC coating prepared in this paper has a very compact and dense structure, which effectively suppresses the entry of steam and exhibits relatively good high-temperature vapor oxidation resistance of the Zirlo substrate at 1000 °C. In addition, the TiC middle scale effectively hinders inter-elemental diffusion.

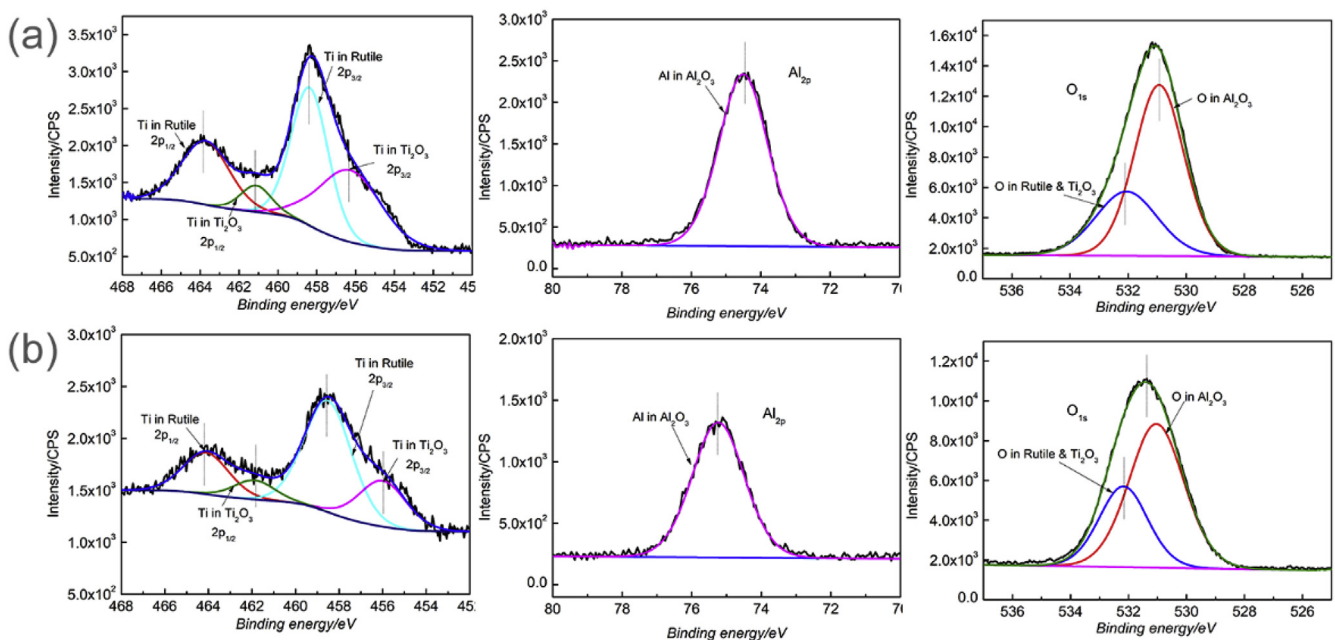


Fig. 7. XPS spectra of Ti<sub>2</sub>AlC-coated Zirlo substrate oxidized at 1000 °C for (a) 10 min and (b) 20 min in steam.

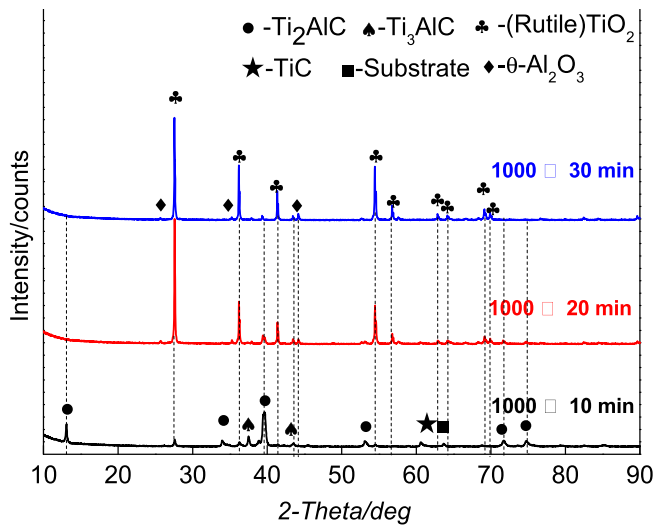


Fig. 8. X-ray diffraction pattern of  $\text{Ti}_2\text{AlC}$  coatings on Zirlo substrate after steam oxidation at  $1000^\circ\text{C}$  for 10 min, 20 min and 30 min.

When the  $\text{Ti}_2\text{AlC}$  coating is oxidized at  $1000^\circ\text{C}$  for 20 min, as shown in Fig. 10a, the thickness of oxide scale increase to  $8.8\mu\text{m}$  and oxide scale with multilayer structure were observed. Combining with EDS elemental mapping (Fig. 10b), it can be seen that the oxide scale mainly consists of three parts, including external Ti- and Al-oxides mixed layer, internal Ti-oxides layer and intermediate Al-oxides. Based on the XRD and XPS results, the order of oxide from surface to inner is a mixed layer of  $\text{R-TiO}_2$  and  $\alpha\text{-Al}_2\text{O}_3$ ,  $\alpha\text{-Al}_2\text{O}_3$  layer and porous  $\text{R-TiO}_2$  layer. Meanwhile,  $\text{Zr-Al}$  diffused layer appears at the interface between coating and substrate. The  $\text{Ti}_2\text{AlC}$  coating is not completely oxidized at this time, leaving about  $6.4\mu\text{m}$ , and the Zirlo substrate is not oxidized. In fact, in order to obtain excellent high temperature oxidation

resistance of  $\text{Ti}_2\text{AlC}$  coating during oxidation, it is prerequisite to form a compact and thick  $\text{Al}_2\text{O}_3$  layer. However, the formed  $\alpha\text{-Al}_2\text{O}_3$  layer here by oxidation at  $1000^\circ\text{C}$  for 20 min is relatively thin, which is mainly limited by the short diffusion time of Al.

In order to obtain thicker  $\text{Al}_2\text{O}_3$  layer and further study the high temperature vapor oxidation resistance of  $\text{Ti}_2\text{AlC}$ -coated Zirlo substrate. Fig. 10c shows SEM images of cross-section of  $\text{Ti}_2\text{AlC}$  coated Zirlo substrate after 30 min oxidation. The results show that the whole coating has been consumed, forming an oxide layer with a thickness of about  $20\mu\text{m}$ , and the substrate has also undergone slight oxidation. It can be seen that the oxide scale also exhibits three layers structure. At this time, the thickness of the  $\text{Al}_2\text{O}_3$  intermediate layer increases. However, a small amount of  $\text{TiO}_2$  is formed in the intermediate layer of  $\text{Al}_2\text{O}_3$ , and the  $\text{Al}_2\text{O}_3$  layer becomes loose. Meanwhile, the morphology of porous  $\text{TiO}_2$  becomes loose.

On the one hand, Al diffuses over a long distance with the increase of oxidation time, resulting in an increase in the thickness of the formed  $\text{Al}_2\text{O}_3$  layer. On the other hand, a large amount of Al diffused into the substrate as shown in EDS elemental mapping (Fig. 10d), the structure of  $\text{Ti}_2\text{AlC}$  phase is destroyed and the diffusion of Al from coating interior to surface is inhibited. This is also the reason why the coating is rapidly consumed after oxidation in steam for 30 min, which is called breakaway oxidation [7]. Li et al. [34] pointed out that catastrophic breakaway oxidation would occur when bulk  $\text{Ti}_3\text{AlC}_2$  was oxidized at  $1100^\circ\text{C}$  for 4000 h, correspondingly, and the oxidation kinetics transformed from cubic law to linear law. Therefore, similar phenomenon also exists in our work. According to the phenomenon of breakaway oxidation, it can be predicted that the oxidation rate will be accelerated with the prolongation of oxidation time. In the future, the preparation of a thicker  $\text{Ti}_2\text{AlC}$  coating and a better diffusion barrier are necessary for further prolonging the oxidation time under steam atmosphere at  $1000^\circ\text{C}$ .

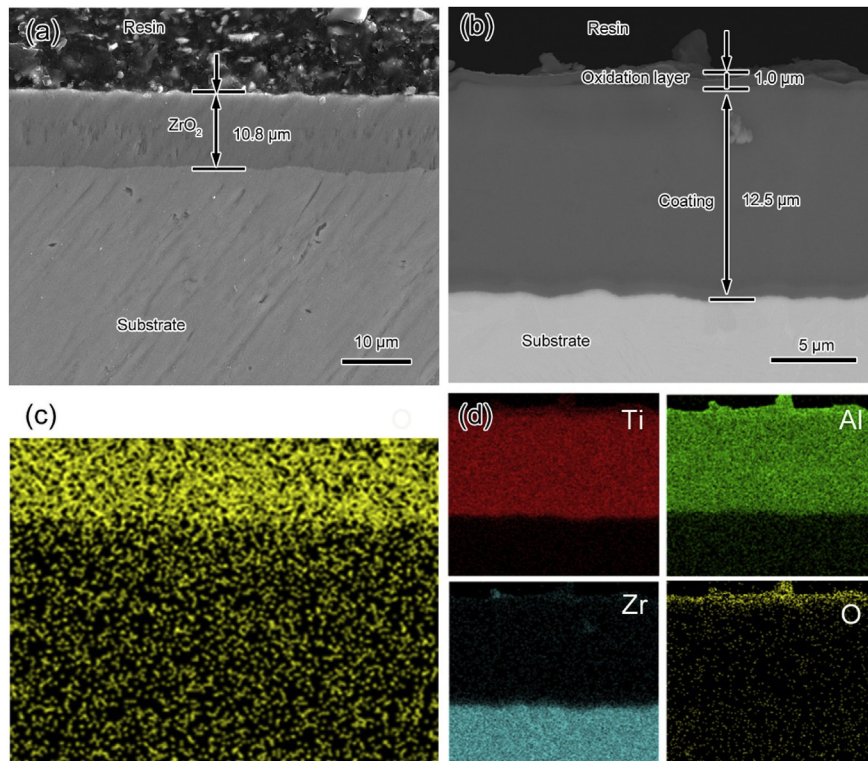
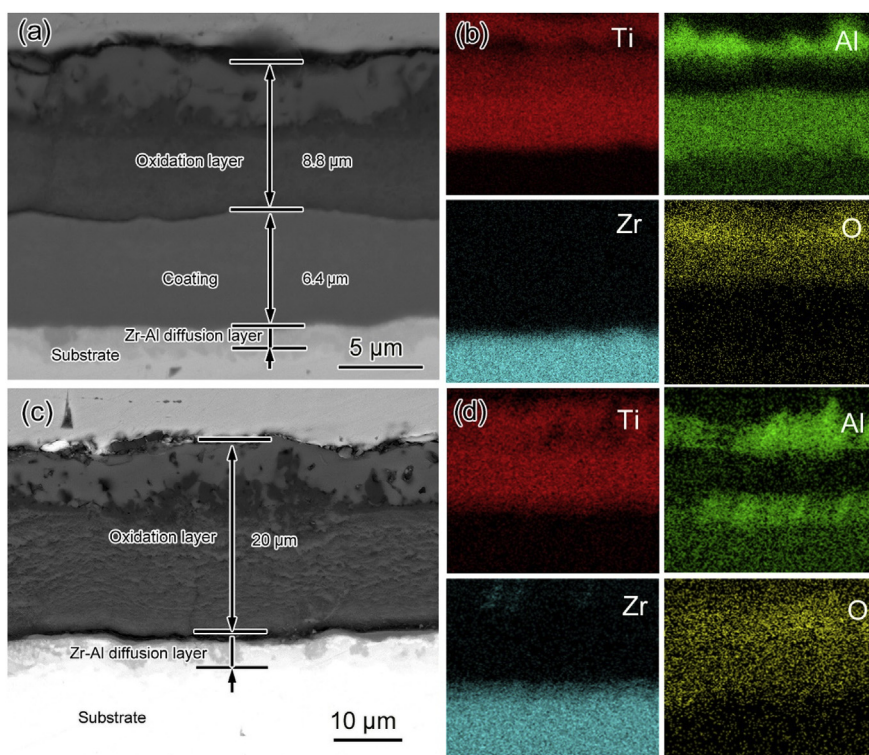


Fig. 9. Cross-section images of both bare Zirlo substrate (a) and  $\text{Ti}_2\text{AlC}$ -coated Zirlo substrate (b) oxidized at  $1000^\circ\text{C}$  for 10 min with the corresponding EDS elemental mapping (c) and (d), respectively.



**Fig. 10.** SEM images of cross section of coated samples after oxidation at 1000 °C for 20 min (a) and 30 min (c) with corresponding EDS elemental mapping (b) and (d), respectively.

### 3.2.2. 1100 °C and 1200 °C oxidation resistance in steam

In addition to prolonging the oxidation time, increasing the temperature will also exert serious influence on the oxidation of samples.

Fig. 11 clearly show that surface appearance of the samples after isothermal oxidation in steam at 1100–1200 °C for different times with corresponding change of the oxidation weight gain. Compared with oxidation performance at 1000 °C for 10 min, local corrosion occurred on the surface of samples after oxidation at 1100 °C for 10 min and the weight gain increase to 1.94 g/cm<sup>2</sup>, demonstrating a more serious oxidation occurs as oxidation temperature increase to 1100 °C. When oxidation is conducted at 1200 °C for 5 min, the coating surface remains intact and can maintain a relatively low weight gain (1.17 g/cm<sup>2</sup>). However, the oxide layer has peeled off and the weight gain (16.65 g/cm<sup>2</sup>) increases significantly after 10 min at 1200 °C.

Fig. 12 presents the surface morphologies of sample oxidized at 1100–1200 °C. After oxidation at 1100 °C for 10 min (Fig. 12a and d), the surface morphology is the same as that of oxidation at 1000 °C for

20 min and 30 min. However, when the oxidation temperatures rise to 1200 °C (Fig. 12b and e), the grain size of TiO<sub>2</sub> becomes larger, and the oxidation products become denser. After oxidation at 1200 °C for 10 min, as shown in Fig. 12c and f, it is obvious that the TiO<sub>2</sub> oxides have a bigger grain size and denser surface.

The XRD measurements (Fig. 13) show that, when the sample is oxidized at both 1100 °C for 10 min and 1200 °C for 5 min, the diffraction peaks is still mainly R-TiO<sub>2</sub> and α-Al<sub>2</sub>O<sub>3</sub>, with a small amount of Ti<sub>2</sub>AlC. However, when the oxidation time is extended to 10 min at 1200 °C, all diffraction peaks change to ZrO<sub>2</sub>, which indicates that all the oxidation products have been exfoliated and the substrate has also suffered oxidation.

Fig. 14 displays SEM images of surface and cross-section of bare and Ti<sub>2</sub>AlC coated samples after oxidation at 1100 °C for 10 min with corresponding EDS elemental mapping results. The results are similar to those obtained after oxidation at 1000 °C for 20 min. In addition to the formation of three-layer oxide, there is a residual Ti<sub>2</sub>AlC coating with

Oxidation process	1100 °C 10 min	1200 °C 5 min	1200 °C 10 min
Samples (Weight gain)	1.94 mg/cm <sup>2</sup>	1.17 mg/cm <sup>2</sup>	16.65 mg/cm <sup>2</sup> <i>peel off</i>

**Fig. 11.** Surface appearance of the samples after isothermal oxidation in steam at 1100–1200 °C for different times with corresponding change of the oxidation weight gain.

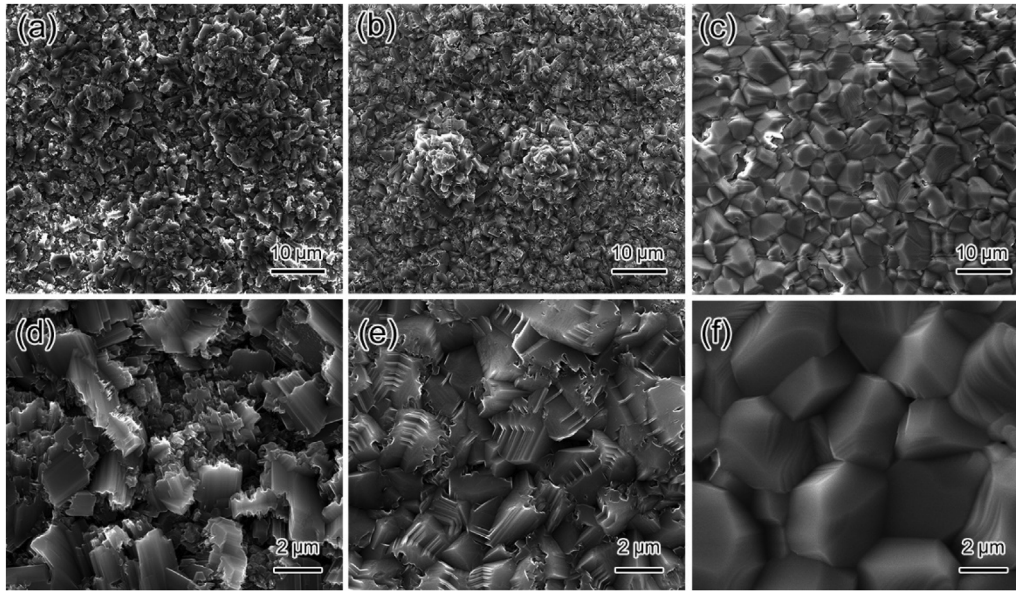


Fig. 12. Surface morphologies of the samples after isothermal oxidation in steam at 1100 °C for 10 min (a), 1200 °C for 5 min (b) and 1200 °C for 10 min (c) with at high magnification (d), (e) and (f), respectively.

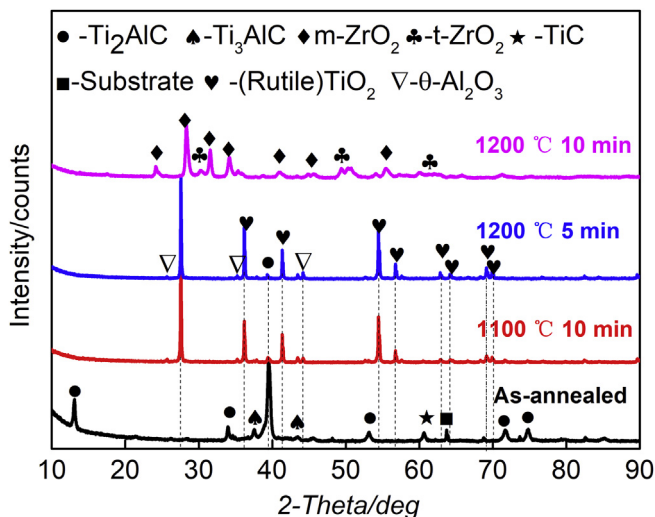


Fig. 13. X-ray diffraction pattern of  $\text{Ti}_2\text{AlC}$  coatings on Zirlo substrate after steam oxidation at 1100 °C for 10 min and 1200 °C for 5 min and 10 min.

the thickness of about 4.4  $\mu\text{m}$ . However, the bare Zirlo itself has been seriously oxidized to a  $\text{ZrO}_2$  layer with the thickness of 26.5  $\mu\text{m}$  (Figs. 14c and 13d). The results reveal that when the oxidation time remains unchanged, the oxidation of  $\text{Ti}_2\text{AlC}$  coating will be accelerated by increasing the oxidation temperature. Nevertheless,  $\text{Ti}_2\text{AlC}$  coating still keeps sufficient protection to the Zirlo substrate.

SEM image of cross-section of  $\text{Ti}_2\text{AlC}$  coated Zirlo substrate after oxidation at 1200 °C for 5 min and 10 min, as depicted in Fig. 15, were conducted, in which the oxides exhibited a loose structure and part of it has fallen off (Fig. 15a). Due to the rapid diffusion of Al to the substrate, a Zr–Al diffusion layer shown in EDS mapping (Fig. 15c) becomes more obvious. Taking severe oxidation conditions into account, the dense structure of  $\text{Ti}_2\text{AlC}$  coating still effectively inhibits the reaction between steam and Zirlo substrate, which improves the high temperature oxidation resistance of Zirlo substrate in steam at 1200 °C. However, as evidenced from Figs. 15b and 14d, a distinct Zr–O diffusion layer in thickness of 81.1  $\mu\text{m}$  appears and all oxidation products have been exfoliated when the coating was oxidized at 1200 °C for 10 min. The illustration in Fig. 15b shows the surface morphology of the exfoliated

samples, which is a typical  $\text{ZrO}_2$  structure. It can be concluded that with the increase of temperature,  $\text{Ti}_2\text{AlC}$  coatings will undergo very serious oxidation.

### 3.2.3. Mechanism of oxidation resistance

As discussed above, our experimental results focus on the temperature range from 1000 °C to 1200 °C, which is benefit for the considering of real environment of accident tolerance conditions. To better interpret the oxidation results, a schematic diagram is illustrated in Fig. 16. Firstly, the surface coatings are destroyed and oxidized at the highly instantaneous temperature, forming a mixed layer of R– $\text{TiO}_2$  and  $\alpha\text{-Al}_2\text{O}_3$ , as shown in Fig. 16a. The formation of mixed layer has nothing to do with the phase structure of  $\text{Ti}_2\text{AlC}$  MAX phase itself and the bonding mode between atoms. It is mainly related to the content of steam. Secondly, the Ti–Al bonds in  $\text{Ti}_2\text{AlC}$  phase break preferentially under thermal driving, and Al diffuse to both the surface and substrate simultaneously. One of the key reasons contributing to the excellent high-temperature oxidation resistance of  $\text{Ti}_2\text{AlC}$  MAX phase is its nanolaminated microstructure, in which the  $\text{Ti}_2\text{C}$  layers being interleaved with single Al layers. Because of the weak bonding energy between Al and Ti in the structure, the Al atomic easily diffuses from the inside of the coating to the surface layer, leaving a  $\text{Ti}_2\text{C}$  layer. The Al and  $\text{Ti}_2\text{C}$  layer, respectively, react with steam diffused into the interior of the coating to form an  $\alpha\text{-Al}_2\text{O}_3$  layer and a porous R– $\text{TiO}_2$  layer. The oxidation process is controlled by Al diffusion under thermal driving. The pore in the  $\text{TiO}_2$  layer is mainly due to the formation of  $\text{CO}_2$  and  $\text{H}_2$  in the reaction process. Schematic diagram of the final oxidation results is shown in Fig. 16b.

Based on the experimental results of oxidation at 1000–1200 °C in steam, it indicates that, even though  $\text{Ti}_2\text{AlC}$  coating with the characteristics of compactness, considerable thickness and less arc particles were successfully obtained in our study by a hybrid arc/magnetron sputtering and post-annealing method, it is very difficult to obtain a continuous and compact  $\text{Al}_2\text{O}_3$  layer during the oxidation process and it is unlikely for coatings to maintain the same high temperature oxidation resistance as bulk materials [35]. The main reasons can be summarized as two points: first, the oxidation resistance of  $\text{Ti}_2\text{AlC}$  coating in steam is limited by the thickness of the coating itself, resulting in insufficient Al content diffusing to the coating surface. Second, a large amount of Al atoms in the coating diffuses into the substrate. Migration of Al leads to collapse of the structure of  $\text{Ti}_2\text{AlC}$  coating, which is one of

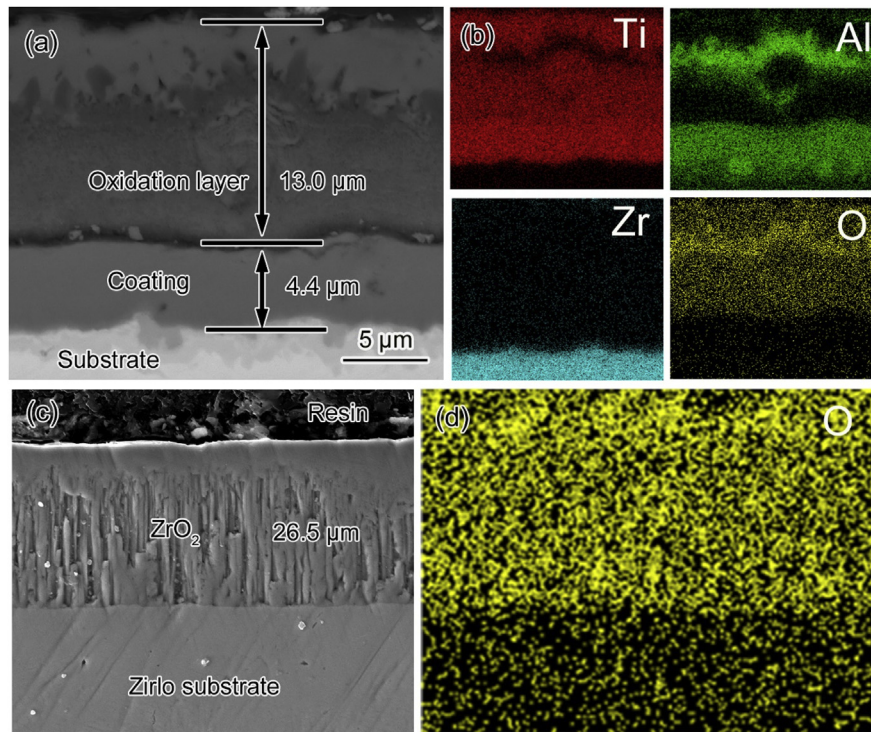


Fig. 14. SEM images of surface and cross-section of bare and Ti<sub>2</sub>AlC coated Zirlo after oxidation at 1100 °C for 10 min with corresponding EDS mapping.

the primary failure mechanisms for the Ti<sub>2</sub>AlC coating and accelerates the oxidation rate of the coating. Of course, the presence of impurities in annealed coatings, Ti<sub>3</sub>AlC, TiC<sub>x</sub> and TiC, may also be responsible for the rapid oxidation of coatings [36]. Although the high temperature oxidation resistance of Ti<sub>2</sub>AlC coating in steam cannot achieve the same effect as the bulk material, it greatly improves the high temperature steam oxidation resistance of the Zirlo substrates at 1000–1200 °C.

#### 4. Conclusion

In the present study, Ti<sub>2</sub>AlC MAX phase coatings, an oxidation resistant material, have been successfully fabricated on Zirlo substrate using hybrid arc/magnetron sputtering followed by post-annealing method. The coating is characterized by high compactness, considerable thickness (12.0 μm) and less marparticles.

The results of high temperature vapor oxidation resistance of both bare and Ti<sub>2</sub>AlC coated Zirlo substrate at 1000–1200 °C proved that,

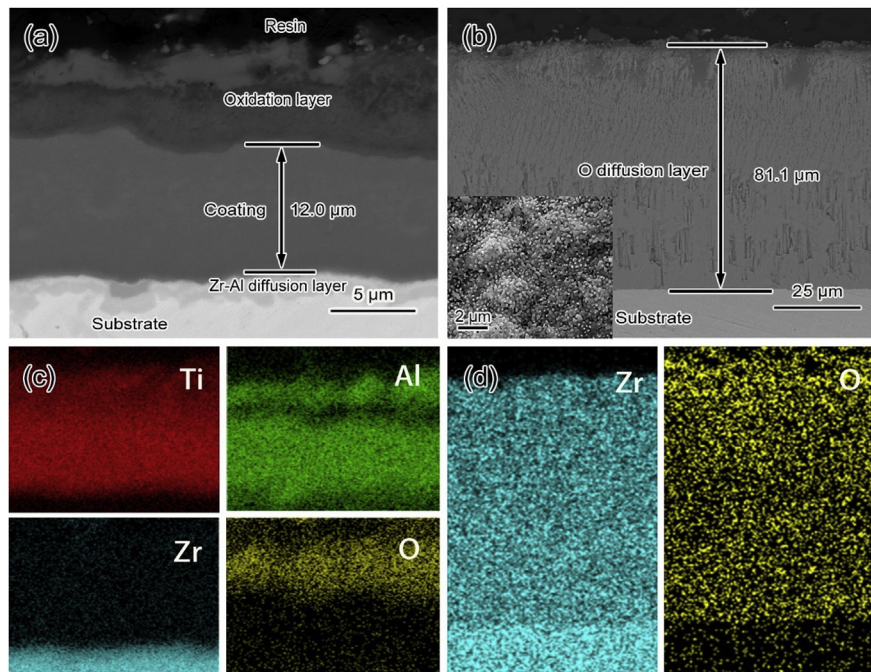


Fig. 15. SEM images of cross section of coated samples after oxidation at 1200 °C for 5 min and 10 min, respectively, with corresponding EDS elemental mapping.

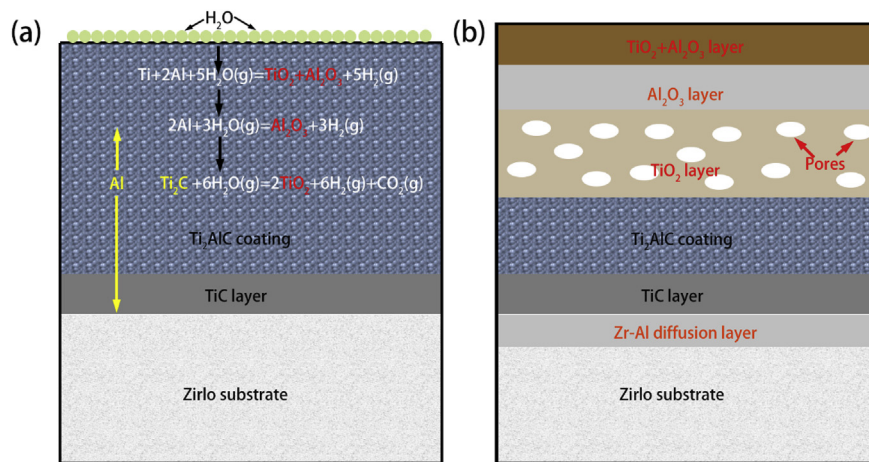


Fig. 16. Schematic diagram of cross-sectional microstructure of  $\text{Ti}_2\text{AlC}$  coated Zirlo substrate oxidized at 1000–1200 °C, (a) oxidation process and (b) result.

because of the dense structure of  $\text{Ti}_2\text{AlC}$  coating itself and the formation of three oxide layers during oxidation, the coating effectively prevented the reaction between steam and zirconium alloy. Furthermore, the  $\text{Ti}_2\text{AlC}$  coating improved the high temperature vapor oxidation resistance of Zirlo substrate. With the increase of oxidation temperature and time, the oxidation of  $\text{Ti}_2\text{AlC}$  coating will be intensified. A large amount of Al diffusion to the Zirlo substrate was proposed as the main cause of coating failure and rapid consumption.

The results bring forward the promising possibilities for the application of MAX phase coatings as ATF cladding coating materials. In order to further improve the high temperature oxidation resistance of Zirlo in steam and apply it in LOCA conditions, however, it is further essential to prepare thicker coatings and a suitable diffusion barrier. Taking this concept and the great contribution from surface coating technology, it should be pointed out that the hybrid arc/magnetron sputtering provides a facile strategy to fabricate the MAX phase coatings as oxidation protective candidates for ATF claddings.

### Acknowledgements

This work was financially supported by the National Natural Science Foundation of China (51875555), China Postdoctoral Science Foundation (2018M632513), and Zhejiang Provincial Natural Science Foundation (LQ19E010002).

### References

- [1] A. Shibata, Y. Kato, T. Taguchi, M. Futakawa, K. Maekawa, Corrosion properties of zircaloy-4 and M5 under simulated PWR water conditions, *Nucl. Technol.* 196 (2017) 89–99.
- [2] D.J. Park, H.G. Kim, Y.I. Jung, J.H. Park, J.H. Yang, Y.H. Koo, Behavior of an improved Zr fuel cladding with oxidation resistant coating under loss-of-coolant accident conditions, *J. Nucl. Mater.* 482 (2016) 75–82.
- [3] C. Tang, M. Stueber, H.J. Seifert, M. Steinbrueck, Protective coatings on zirconium-based alloys as accident tolerant fuel (ATF) claddings, *Corros. Res.* 35 (2017).
- [4] K. Lee, D. Kim, Y.S. Yoon, SiC/Si thin film deposited on zircaloy to improved accident tolerant fuel cladding, *Thin Solid Films* 660 (2018) 221–230.
- [5] W. Bao, J. Xue, J.X. Liu, X. Wang, Y. Gu, F. Xu, G.J. Zhang, Coating SiC on Zircaloy-4 by magnetron sputtering at room temperature, *J. Alloy. Comp.* 730 (2018) 81–87.
- [6] J.H. Park, H.G. Kim, J.Y. Park, Y.I. Jung, D.J. Park, Y.H. Koo, High temperature steam-oxidation behavior of arc ion plated Cr coatings for accident tolerant fuel claddings, *Surf. Coating. Technol.* 280 (2015) 256–259.
- [7] I. Gurrappa, S. Weinbruch, D. Naumenko, W.J. Quadackers, Factors governing breakaway oxidation of FeCrAl-based alloys, *Mater. Corros.* 51 (2000) 224–235.
- [8] W. Zhang, R. Tang, Z.B. Yang, C.H. Liu, H. Chang, J.J. Yang, J.L. Liao, Y.Y. Yang, N. Liu, Preparation, structure, and properties of an AlCrMoNbZr high-entropy alloy coating for accident-tolerant fuel cladding, *Surf. Coating. Technol.* 347 (2018) 13–19.
- [9] R. Shu, F. Ge, F. Meng, P. Li, J. Wang, Q. Huang, P. Eklund, F. Huang, One-step synthesis of polycrystalline  $\text{V}_2\text{AlC}$  thin films on amorphous substrates by magnetron co-sputtering, *Vacuum* 146 (2017) 106–110.
- [10] Z. Wang, X. Li, J. Zhou, P. Liu, Q. Huang, P. Ke, A. Wang, Microstructure evolution of V-Al-C coatings synthesized from a  $\text{V}_2\text{AlC}$  compound target after vacuum annealing treatment, *J. Alloy. Comp.* 661 (2016) 476–482.
- [11] C. Tang, M. Steinbrueck, M. Stueber, M. Grosse, X. Yu, S. Ulrich, H.J. Seifert, Deposition, characterization and high-temperature steam oxidation behavior of single-phase  $\text{Ti}_2\text{AlC}$ -coated Zircaloy-4, *Corros. Sci.* 135 (2018) 87–98.
- [12] M.W. Barsoum, The  $\text{M}_{N+1}\text{AlX}_N$  phases: a new class of solids; thermodynamically stable nanolaminates, *Prog. Solid State Chem.* 28 (2000) 201–281.
- [13] P. Eklund, M. Beckers, U. Jansson, H. Högberg, L. Hultman, The  $\text{M}_{N+1}\text{AlX}_N$  phases: materials science and thin-film processing, *Thin Solid Films* 518 (2010) 1851–1878.
- [14] E.N. Hoffman, D.W. Vinson, R.L. Sindelar, D.J. Tallman, G. Kohse, M.W. Barsoum, MAX phase carbides and nitrides: properties for future nuclear power plant in-core applications and neutron transmutation analysis, *Nucl. Eng. Des.* 244 (2012) 17–24.
- [15] K. Luo, X.H. Zha, Q. Huang, C.-T. Lin, R. Zhang, S. Du, Theoretical investigations on helium trapping in the Zr/ $\text{Ti}_2\text{AlC}$  interface, *Surf. Coating. Technol.* 322 (2017) 19–24.
- [16] S. Basu, N. Obando, A. Gowdy, I. Karaman, M. Radovic, Long-term oxidation of  $\text{Ti}_2\text{AlC}$  in air and water vapor at 1000–1300 °C temperature range, *J. Electrochem. Soc.* 159 (2012) C90.
- [17] C. Tang, M. Steinbrueck, M. Grosse, T. Bergfeldt, H.J. Seifert, Oxidation behavior of  $\text{Ti}_2\text{AlC}$  in the temperature range of 1400 °C–1600 °C in steam, *J. Nucl. Mater.* 490 (2017) 130–142.
- [18] B. Maier, H. Yeom, G. Johnson, T. Dabney, J. Walters, J. Romero, H. Shah, P. Xu, K. Sridharan, Correction to: development of cold spray coatings for accident-tolerant fuel cladding in light water reactors, *J. Occup. Med.* 70 (2018) 248–248.
- [19] C. Tang, M. Klimentov, U. Jaentsch, H. Leiste, M. Rinke, S. Ulrich, M. Steinbrueck, H.J. Seifert, M. Stueber, Synthesis and characterization of  $\text{Ti}_2\text{AlC}$  coatings by magnetron sputtering from three elemental targets and ex-situ annealing, *Surf. Coating. Technol.* 309 (2017) 445–455.
- [20] J. Fu, T.F. Zhang, Q. Xia, S.H. Lim, Z. Wan, T.W. Lee, K.H. Kim, Oxidation and corrosion behavior of nanolaminated MAX-phase  $\text{Ti}_2\text{AlC}$  film synthesized by high-power impulse magnetron sputtering and annealing, *J. Nanomater.* 2015 (2015) 1–12.
- [21] Z. Feng, P. Ke, A. Wang, Preparation of  $\text{Ti}_2\text{AlC}$  MAX phase coating by DC magnetron sputtering deposition and vacuum heat treatment, *J. Mater. Sci. Technol.* 31 (2015) 1193–1197.
- [22] Q.M. Wang, W. Garkas, A.F. Renteria, C. Leyens, H.W. Lee, K.H. Kim, Oxidation behaviour of Ti-Al-C films composed mainly of a  $\text{Ti}_2\text{AlC}$  phase, *Corros. Sci.* 53 (2011) 2948–2955.
- [23] B.R. Maier, B.L. Garcia-Diaz, B. Hauch, L.C. Olson, R.L. Sindelar, K. Sridharan, Cold spray deposition of  $\text{Ti}_2\text{AlC}$  coatings for improved nuclear fuel cladding, *J. Nucl. Mater.* 466 (2015) 712–717.
- [24] C. Tang, M. Steinbrueck, M. Stueber, M. Grosse, X. Yu, S. Ulrich, H.J. Seifert, Deposition, characterization and high-temperature steam oxidation behavior of single-phase  $\text{Ti}_2\text{AlC}$ -coated Zircaloy-4, *Corros. Sci.* 135 (2018) 87–98.
- [25] Z. Wang, J. Liu, L. Wang, X. Li, P. Ke, A. Wang, Dense and high-stability  $\text{Ti}_2\text{AlN}$  MAX phase coatings prepared by the combined cathodic arc/sputter technique, *Appl. Surf. Sci.* 396 (2017) 1435–1442.
- [26] J.J. Li, Y.H. Qian, D. Niu, M.M. Zhang, Z.M. Liu, M.S. Li, Phase formation and microstructure evolution of arc ion deposited  $\text{Cr}_2\text{AlC}$  coating after heat treatment, *Appl. Surf. Sci.* 263 (2012) 457–464.
- [27] W.T. Li, Z.W. Wang, D. Zhang, J. Pan, P. Ke, A. Wang, Preparation of  $\text{Ti}_2\text{AlC}$  MAX phase coating by the combination of a hybrid cathode arc/magnetron sputtering with post-annealing, *Acta Metall. Sin.* (2018), <https://doi.org/10.11900/0412.1961.2018.00285>.
- [28] W.C. Oliver, G.M. Pharr, AN IMPROVED TECHNIQUE FOR DETERMINING HARDNESS AND ELASTIC-MODULUS USING LOAD AND DISPLACEMENT SENSING INDENTATION EXPERIMENTS, *J. Mater. Res.* 7 (1992) 1564–1583.
- [29] V. Presser, M. Naguib, L. Chaput, A. Togo, G. Hug, M.W. Barsoum, First-order Raman scattering of the MAX phases:  $\text{Ti}_2\text{AlN}$ ,  $\text{Ti}_2\text{AlC}_{0.5}\text{N}_{0.5}$ ,  $\text{Ti}_2\text{AlC}$ ,  $(\text{Ti}_{0.5}\text{V}_{0.5})_2\text{AlC}$ ,  $\text{V}_2\text{AlC}$ ,  $\text{Ti}_3\text{AlC}_2$ , and  $\text{Ti}_3\text{GeC}_2$ , *J. Raman Spectrosc.* 43 (2012) 168–172.
- [30] I. Younker, M. Fratoni, Neutronic evaluation of coating and cladding materials for

- accident tolerant fuels, *Prog. Nucl. Energy* 88 (2016) 10–18.
- [31] A.M.A. Leyland, On the significance of the H/E ratio in wear control: a nano-composite coating approach to optimised tribological behaviour, *Wear* 246 (2000) 1–11.
- [32] K.L. Johnson, *Contact Mechanics*, Cambridge University Press, 1985 452.
- [33] P. Pérez, On the influence of water vapour on the oxidation behaviour of pure Ti, *Corros. Sci.* 49 (2007) 1172–1185.
- [34] X. Li, L. Zheng, Y. Qian, J. Xu, M. Li, Breakaway oxidation of  $Ti_3AlC_2$  during long-term exposure in air at 1100 °C, *Corros. Sci.* 104 (2016) 112–122.
- [35] S. Basu, N. Obando, A. Gowdy, I. Karaman, M. Radovic, Long-term oxidation of  $Ti_2AlC$  in air and water vapor at 1000–1300 °C temperature range, *J. Electrochem. Soc.* 159 (2012) C90–C96.
- [36] M. Sonestedt, J. Frodelius, M. Sundberg, L. Hultman, K. Stiller, Oxidation of  $Ti_2AlC$  bulk and spray deposited coatings, *Corros. Sci.* 52 (2010) 3955–3961.